Two-photon excitation of the metastable 2*s* state of hydrogen assisted by laser-induced chirped Stark shifts and continuum structure

L. P. Yatsenko,* V. I. Romanenko,* B. W. Shore,† T. Halfmann, and K. Bergmann
Fachbereich Physik der Universität, D-67653 Kaiserslautern, Germany
(Received 14 December 2004; published 31 March 2005)

Traditional two-photon excitation suffers from two difficulties that prevent complete population transfer: dynamic Stark shifts and multiphoton ionization. We describe a technique for overcoming these limitations by using a second field to control dynamic Stark shifts via Stark-chirped rapid adiabatic passage (SCRAP) and *simultaneously* suppress undesired photoionization via laser-induced continuum structure (LICS). We illustrate this proposed procedure by numerical simulations of two-photon excitation of the metastable 2*s* state of hydrogen, showing that efficient excitation can be expected when the two laser pulses are properly crafted.

DOI: 10.1103/PhysRevA.71.033418 PACS number(s): 32.80.Rm, 34.50.Rk

I. INTRODUCTION

The long lifetime (0.12 s) and high internal excitation energy (10 eV) of the metastable 2*s* state of hydrogen has long attracted interest of experimenters, while the simple internal structure continues to hold interest of theoreticians. This metastable state is of interest for use in precision spectroscopy of transitions starting from the 2*s* state and for improved accuracy in determining fundamental constants, e.g., the Lamb shift and the Rydberg constant [1,2]. Precision measurements of hyperfine splitting in 2*s* are desirable for the information they give on a combination of proton structure and QED [3].

The metastable state 2*s* is nearly degenerate with the 2*p* states, and so the excitation is readily quenched, with production of Lyman-alpha radiation, either by collisions or by weak electric fields that mix the two states [4]. It may therefore be useful as a source of Lyman-alpha radiation for high-resolution spectroscopy [5]. The high internal energy of excited hydrogen atoms makes these attractive for detecting single atoms by electron multipliers [1].

The theoretical simplicity of atomic hydrogen makes this a desirable species for studying basic collision phenomena, and so these states have been the subject of atomic beam studies of collision phenomena—e.g., collision-induced ionization, reactive scattering, and molecular dissociation processes. Theoretical understanding and modeling of such experiments using hydrogen are much simpler than for multi electron atoms, for the quantum-mechanical properties of the hydrogen atom can be analytically treated. Nevertheless, accurate description of the collision cross sections between H(2*s*) and H(1*s*) remains a challenge for theory [1]. A source of H(2*s*) would be of use for verifying theoretical predictions of cross sections for dissociative ionization and double excitation transfer in H(2*s*)−H(2*s*) collisions [6] and to verify calculations of long-range H(2*s*)−H(2*s*) interaction potential [5]. The density dependence of the frequency of the two-photon $1s-2s$ transition is an important diagnostic in Bose-Einstein condensation [7].

Thus there has long been a need for techniques that prepare sources of metastable hydrogen. The most common technique has been to pass a beam of hydrogen molecules through an electric discharge, where electron collisions induce dissociation and excitation [2,3]. Charge exchange between protons and vapor has also been used [8]. More recently optical pumping techniques have been used, with laser excitation of the $1s-3p$ transition using Lyman-beta radiation followed by spontaneous radiative cascade from the 2*s* state [2]. A technique using Stark-chirped rapid adiabatic passage (SCRAP), suggested earlier [9–12], is an important element in the present proposal. We here suggest significant modification of that technique for efficient excitation to the 2*s* state from the ground 1*s* state of hydrogen. The procedure involves a sequence of overlapping pulses of two frequencies which together overcome some of the limitations of the previous proposal.

To place the present proposal into context Fig. 1 shows linkage patterns for three schemes of laser excitation: (a) straightforward resonant two-photon excitation (inevitably accompanied by photoionization) produced by the single pulse *P*; (b) the SCRAP procedure using three laser pulses P_1, P_2, and *S* proposed earlier [9]; and (c) the present proposal using two laser pulses, *P* and *S*.

We note that other multifrequency proposals for similar population transfer or inversion have been proposed. One proposal combined steady strong two-photon excitation with a second steady linkage to an autoionizing resonance in the photoionization continuum [13]. A recent proposal, aimed at producing population transfer in sodium dimers, uses three delayed pulses to produce rapid adiabatic passage while suppressing photodissociation through laser-induced continuum structure LICS [14]. The use of a two-pulse sequence, in the presence of a third "dressing" field, has been proposed as a means of producing coherent control of dissociation (or photoionization) products during adiabatic passage, i.e., suppression of one continuum while enhancing another [15].

*Permanent address: Institute of Physics, Ukrainian Academy of Sciences, prospect Nauki 46, Kiev-28, 03028, Ukraine.
†Permanent address: 618 Escondido Cir., Livermore, CA 94550, USA.

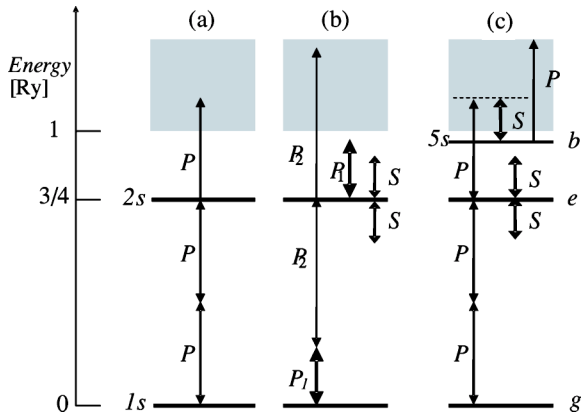

FIG. 1. Schematic diagram of energy levels (in Rydbergs) showing dipole-coupling linkages for possible excitation schemes for producing 2*s* population of hydrogen using laser pulses. (a) Resonant two-photon excitation accompanied by (detrimental) photoionization ($\lambda_P = 243.1$ nm). (b) Using two different laser pulses P_1 and P_2 to produce a two-photon transition ($\lambda_{P_1} = 399.5$ nm, $\lambda_{P_2} = 174.8$ nm), with a third Stark-shifting laser S ($\lambda_S = 1064$ nm). (c) A single laser P used for the two-photon transition ($\lambda_P = 243.1$ nm), with a second laser S producing Stark shifts and LICS ($\lambda_S = 552.5$ nm). In (b) and (c) the two photons are detuned from the 1*s*–2*s* transition resonance, but by too little to be shown here. The state labels *g*, *e*, and *b* used in the present work appear at the right.

II. DESCRIPTION OF THE SUGGESTED TECHNIQUE

The preparation of metastable states of atoms, in particular H(2*s*), by radiative excitation through a two-photon transition, though highly desirable as a practical tool, suffers from two well-known problems. First, the presence of a field of sufficient strength to produce appreciable population transfer will inevitably cause other two-photon processes. In particular, laser-induced Stark shifts are, like the desired two-photon transition, directly proportional to laser intensity. These time-dependent shifts make it difficult to establish and maintain the needed two-photon resonance conditions.

Second, because the metastable state is typically highly excited, the absorption of a third laser photon may readily ionize the target metastable state [see Fig. 1(a)] thereby diminishing the resulting population transfer.

Each of these individual handicaps has been separately overcome. The unavoidable dynamic Stark shifts that accompany any conventional two-photon process can be counteracted by use of a second field, nonresonant, that produces a carefully timed sweep of adiabatic energies. This procedure, demonstrated experimentally and described theoretically, has been termed Stark-chirped rapid adiabatic passage (SCRAP) [9–12]. The photoionization loss that will inevitably accompany any laser field of sufficiently short wavelength has been suppressed with the aid of laser-induced continuum structure (or "pseudoautoionizing state"), a technique that can, in principle create a narrow transparency window in the variation of the photoionization cross section versus frequency.

The following subsections summarize these two individual mechanisms, SCRAP and LICS. We propose to combine them, using only two pulsed fields, as described in subsequent sections.

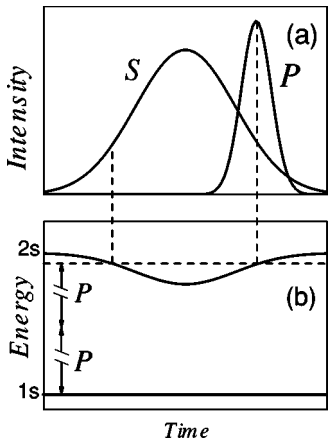

FIG. 2. The SCRAP procedure: (a) Pulse sequence of intensities showing long Stark-shifting pulse *S* and shorter two-photon excitation pulse *P*. (b) The energies of 1*s* and 2*s* states subject to Stark shifts induced by the *S* laser, showing times of resonance with two-photon excitation (dashed vertical lines).

A. The SCRAP technique

Our proposed implementation of the SCRAP method is based on the coordinated interaction of the atom with two suitably delayed pulsed laser fields, termed *P* and *S*. The *S* laser, typically an infrared laser, induces Stark shifts of the 1*s* and 2*s* levels, while the *P*-laser field drives a two-photon transition between the 1*s* and 2*s* states. The *P* laser is slightly detuned from the two photon resonance; the detuning is of the order of, but less than, the maximum Stark shift induced by the *S* laser.

The Stark-shifting *S* laser drives the $1s-2s$ transition frequency twice through resonance with the two photons of the *P* laser: first during the rise of the *S* pulse and second when the *S*-pulse intensity decreases. For optimum performance of the SCRAP technique the *P*-laser pulse should have a slightly shorter pulse duration than the *S* laser pulse and should be delayed so as to reach maximum intensity at a time when the two-photon resonance condition is met. The result of the combined action of the two pulses is a Landau-Zener-type adiabatic passage whereby the atom undergoes a transition from the 1*s* to the 2*s* state. Adiabatic passage occurs only at one of the resonances, since the *P*-laser intensity is too small (ideally zero) at the other resonance. Figure 2 shows the operation of this general idea applied to the 1*s*–2*s* transition.

In the previous implementation of the SCRAP technique [9], schematically indicated in Fig. 1(b), the excitation step used two concurrent pulses (P_1 and P_2) of different frequencies in order to reduce detrimental photoionization of the 2*s* state: a strong field of frequency too low (wavelength $\lambda_{P_1} = 399.5$ nm) to produce photoionization loss, and a weak field whose frequency was sufficiently high (wavelength $\lambda_{P_2} = 174.8$ nm) that photoionization was into the continuum well above threshold, where the photoionization cross section is small. With such an approach the desired two-photon transition is driven mainly by the strong low-frequency field, while photoionization occurs only by the weak high-frequency field. Simulations have predicted good population

transfer (up to 98%) when these two laser fields, plus a third Stark-shifting laser, are used [9]. However, there are practical difficulties implementing this scheme because it requires a very short wavelength laser (174.8 nm). Thus there remains interest in finding an alternative procedure for efficiently populating this metastable state.

B. Ionization suppression by LICS

The mechanism for suppression of photoionization at a preselected frequency is based on creating a resonance structure in the photoionization continuum such that there occurs, at the chosen frequency, destructive interference between various ionization pathways—an effect similar to that seen in autoionization and described by a Fano profile [16]. This laser-induced continuum structure (LICS) has been discussed for 30 years [17] and has been demonstrated in many experiments [18,19]. Numerous theoretical papers have presented the complete theory for the effect [20,21] and it has been extensively reviewed [22]. (For more recent references, see Ref. [14].) Under favorable conditions it can substantially suppress the photoionization that would otherwise be produced by the excitation laser [19].

The possibility of using LICS to enhance two-photon excitation of the 2*s* state in hydrogen has been considered by Dörr *et al.* [23] who simulated the use of two laser pulses of different frequencies to transfer population from the 1*s* state to the 2*s* state via the continuum. They predicted that, at most, 17% of the population could be found in the 2*s* state at the end of the pulse. In addition to the low efficiency of this proposed approach, it would require an inconvenient laser wavelength shorter than 90 nm.

C. Combining SCRAP with LICS: A three-level model

We here describe how to implement a combination of SCRAP and LICS using only two laser fields. We demonstrate, using numerical simulation, that this is a practical scheme for efficient preparation of the metastable 2*s* state of hydrogen, via single-frequency two-photon adiabatic transition from the 1*s* ground state.

Figure 1(c) shows an idealized level scheme of the hydrogen atom. A two-photon transition, involving a pulsed laser field P of constant carrier frequency ω_P (and wavelength near 243 nm) links the ground state g of energy E_g (the 1*s* state for hydrogen) with a metastable excited state e of energy E_e (the 2*s* state for hydrogen) via two-photon transition. The P field also photoionizes the bound state b, into a continuum at energy $E_c = E_b + \hbar\omega_P$, with the rate $\Gamma_{bP}(t)$. As required for SCRAP, we intentionally introduce an initial frequency mismatch, parametrized by the detuning Δ_P defined by the equation

$$\hbar\Delta_P = 2\hbar\omega_P - (E_e - E_g). \tag{1}$$

We introduce a second pulsed laser field S of carrier frequency ω_S, to connect the continuum at energy E_c, as reached by a three-photon process of the P field, to a particular bound state b, of energy E_b (the 5*s* state for hydrogen). The needed wavelength is around 552 nm. The detuning from the resonance for this transition is defined through the equation

$$\hbar\Delta_{PS} = \hbar(\omega_S - \omega_P) - (E_e - E_b). \tag{2}$$

The S field frequency is insufficient to photoionize state e in a single step, but it can produce two-photon ionization, with the rate $\Gamma_{e2S}(t)$. The P and S fields can each photoionize state b, with rates $\Gamma_{bP}(t)$ and $\Gamma_{bS}(t)$, respectively.

Laser pulses with the needed wavelengths and intensities are readily obtained from commercial laser systems. Frequency doubling of pulsed ns lasers conveniently provides 1–2 mJ at a wavelength of 243 nm. Intensity of 2 GW/cm^2, as required for the P field, is obtained by focusing this laser to a 100-μm-diameter spot. The S laser, at wavelength 552 nm, requires no frequency conversion. The needed wavelengths and intensities are readily obtained from commercial laser systems.

D. The Hamiltonian

As has been shown in theoretical treatments of LICS [20] the continuum states can be adiabatically eliminated to produce a three-state system in which there is no reference to the continuum. The state vector then has the expansion

$$\Psi(t) = \exp[-i\zeta_g(t)]C_g(t)\psi_g + \exp[-i\zeta_e(t)]C_e(t)\psi_e + \exp[-i\zeta_b(t)]C_b(t)\psi_b, \tag{3}$$

where $\psi_n(n=g,e,b)$ are the bare quantum states in the absence of laser fields and the $\zeta_n(t)$ are time-dependent phases chosen to enable the rotating-wave approximation. The resulting Schrödinger equation reads, in matrix form, $(d/dt)\mathbf{C}(t) = -i\mathsf{W}(t)\mathbf{C}(t)$, where the effective Hamiltonian is (see the Appendix)

$$\mathsf{W}(t) = \frac{1}{2}\begin{bmatrix} 2S_g(t) + 2\Delta_P & \Omega_P(t) & 0 \\ \Omega_P(t) & 2S_e(t) - i\Gamma_e(t) - i\gamma_e & -(i+q)\Omega_{SP}(t) \\ 0 & -(i+q)\Omega_{SP}(t) & 2S_b(t) + 2\Delta_{PS} - i\Gamma_b(t) - i\gamma_b \end{bmatrix}. \tag{4}$$

The detunings Δ_P and Δ_{PS} are defined by Eqs. (1) and (2). The other quantities appearing here have the following meaning.

The quantity $S_n(t)$ is the dynamic Stark shift of state n, expressible as the sum of a contribution from each of the two fields,

$$S_n(t) = S_{nP}(t) + S_{nS}(t), \quad n = e,g,b. \tag{5}$$

Each contribution is proportional to the related time-dependent laser intensity and to a time-independent but frequency-dependent polarizability.

The photoionization rates from levels e and b are sums of contributions from the two fields,

$$\Gamma_e(t) = \Gamma_{eP}(t) + \Gamma_{e2S}(t), \tag{6}$$

$$\Gamma_b(t) = \Gamma_{bP}(t) + \Gamma_{bS}(t). \tag{7}$$

Here each single-photon rate is proportional to a laser intensity while the two-photon ionization rate Γ_{e2S} is proportional to the square of the S-laser intensity.

The excited states e and b can, in principle, decay by spontaneous emission at rates γ_e and γ_b, respectively. However, in our discussion state e is metastable (lifetime 0.12 s), and so its spontaneous emission decay is negligible. Furthermore, the spontaneous emission rate of state b (lifetime 352 ns) is much smaller than the photoionization rate, so it too can be neglected in the present modeling.

The strength of the coupling between states g and e is parametrized by the two-photon Rabi frequency $\Omega_P(t)$. This is proportional to the intensity of the P laser.

The Hamiltonian of Eq. (4) models the coupling between states e and b through two contributions: by a two-step transition via resonant continuum states [the term $i\Omega_{SP}(t)$], and by Raman-type transitions through nonresonant intermediate discrete and continuum states [the term $q\Omega_{SP}(t)$]. The quantity $\Omega_{SP}(t) \equiv \sqrt{\Gamma_{eP}(t)\Gamma_{bS}(t)}$ is an effective Rabi frequency and the quantity q is the Fano parameter; its value may be calculated from wave functions for bound and continuum states, see Eq. (A12) of the Appendix. The two-photon detuning Δ_{PS} is relevant for the Raman coupling between states b and e resulting from absorption of a photon from the P field and emission of a photon into the S field.

We use the usual nonrelativistic Pauli approximation for the wave functions of the hydrogen atom so all needed atomic parameters (dipole moments, polarizabilities, and photoionization cross sections) can be calculated from analytic expressions with arbitrary numerical accuracy, as described in Ref. [24]. Table I presents the values needed for the numerical simulations reported here.

TABLE I. Theoretical values used in the numerical simulations reported here. All values (other than q) are in ns^{-1} for intensities I_P and I_S in GW/cm^2.

Γ_{eP}	$7.55I_P$	S_{gP}	$-1.7I_P$
Γ_{eS}	0	S_{gS}	$-1.4I_S$
Γ_{bP}	$0.48I_P$	S_{eP}	$8.8I_P$
Γ_{bS}	$7.0I_S$	S_{eS}	$39.5I_S$
Γ_{e2S}	$0.000\,47I_S^2$	S_{bP}	$8.45I_P$
Ω_P	$4.63I_P$	S_{bS}	$44.1I_S$
q	-0.083		

III. NUMERICAL SIMULATION

Two criteria are useful for quantifying the success of any excitation scheme involving probability losses: One is the fraction of the *initial* population that is transferred to the target state e [i.e., the probability $P_e(\infty)$, often termed the excitation efficiency]. The other is the fraction of the *final* population that is found in this state, i.e., the final population *inversion* after the pulses cease. The two criteria have different uses. For example, even though a substantial fraction of the atoms photoionize, it may still be possible to achieve complete population inversion of the atoms remaining unionized at the end of the pulse sequence. Our aim is to exhibit, using solutions of the time-dependent Schrödinger equation to construct probabilities $P_n(t) = |C_n(t)|^2$, conditions of laser intensity and frequency detuning that will maximize either the final population $P_e(\infty)$ in state e—the population transfer—or the final population inversion between states e and g. We quantify this inversion by the fraction

$$\eta \equiv \frac{P_e(\infty) - P_g(\infty)}{P_e(\infty) + P_g(\infty)}. \tag{8}$$

For the simulations we take the P and S pulses to be Gaussian functions,

$$I_P(t) = I_{P\,\max}\exp(-t^2/\tau_P^2),$$

$$I_S(t) = I_{S\,\max}\exp[-(t-t_S)^2/\tau_S^2] \tag{9}$$

with durations τ_P and τ_P, offset in time by the delay t_S, and with peak intensities $I_{P\,\max}$ and $I_{S\,\max}$.

A. Optimal conditions: Theory

To ensure effective and robust population transfer to the state e, the timings of the laser pulses and their static detunings have to be chosen to fulfill both the SCRAP criteria for complete population transfer [9–12] and the LICS criteria for efficient ionization suppression.

The SCRAP technique involves adiabatic evolution of the state vector. In turn, this requires that the temporal area A_P of the P pulse must be sufficiently large,

$$A_P \equiv \int_{-\infty}^{\infty} dt\Omega_P(t) \gg \pi. \tag{10}$$

In order that LICS produce effective ionization suppression the S field must be large and almost constant when the P pulse acts significantly, during the time interval $[-\tau_P, \tau_P]$. This means that the P pulse must be substantially shorter than the S pulse, $\tau_P \ll \tau_S$. Adiabatic passage requires a monotonic change of the Stark shifts (a chirp) during the interval $[-\tau_P, \tau_P]$. The two-photon resonance condition must hold at some moment during this interval. Therefore the time delay t_S has to be larger than τ_P. Although the SCRAP mechanism can succeed with either pulse delayed, in our implementation

the *P* pulse must be delayed with respect to *S* pulse to minimize the two-photon ionization loss.

The detuning of the *P*-laser frequency from the two-photon resonance due to Stark shifts changes roughly linearly with time, at a rate approximately $\Delta_{Stark}/2\tau_P$ where

$$\Delta_{Stark} = S_e(\tau_P) - S_g(\tau_P) - [S_e(-\tau_P) - S_g(-\tau_P)]. \quad (11)$$

For SCRAP to succeed this rate cannot be too large, meaning

$$\Omega_P(0)^2 \gg \frac{\Delta_{Stark}}{\tau_P} \quad (12)$$

and the amplitude of changes cannot be too small, meaning

$$\Omega_P(0) \ll \Delta_{Stark}. \quad (13)$$

When these conditions are not satisfied the SCRAP process fails to produce effective population transfer.

We estimate the optimal value of the *P*-field detuning from two-photon resonance by requiring that exact two-photon resonance occurs at the maximum of the *P* field, i.e., at $t=0$. This choice produces the condition

$$\Delta_{P\ opt} = S_e(0) - S_g(0). \quad (14)$$

Our simulation studies, discussed below, show that this simple expression satisfactorily describes the optimal condition for maximizing population transfer and inversion.

The metastable state undergoes population loss due to photoionization by the *P* field. However, this one-photon ionization can be suppressed, via the LICS mechanism, by proper choice of detuning, $\Delta_{SP}=\Delta_{SP\ opt}$. When all fields are constant the choice

$$\Delta_{SP\ opt} = S_e(0) - S_g(0) - \frac{1}{2}\Gamma_{bS}(0)q \quad (15)$$

completely suppresses single-photon ionization. Our simulation studies show that this expression provides a satisfactory condition for maximizing population transfer with pulsed excitation.

From Eqs. (10) and (12) one might conclude that larger intensities provide more effective population transfer. However, two-photon ionization is present for the entire duration of the pulse. Therefore large intensities produce large two-photon ionization losses, and hence smaller population transfer, although the results become less sensitive to small changes in pulse properties.

B. Optimal conditions: Simulation

To demonstrate the success of our proposed method we integrated the time-dependent Schrödinger equation to obtain the 2*s* population at the conclusion of pulses, $P_e(\infty)$, for a variety of conditions. This section presents some of those results.

Figure 3 shows a contour plot of $P_e(\infty)$, the final population in state *e*, as a function of the two peak intensities $I_{P\ \max}$ and $I_{S\ \max}$. For these and the following calculations the pulse durations τ_S, τ_P and pulse delay t_S are

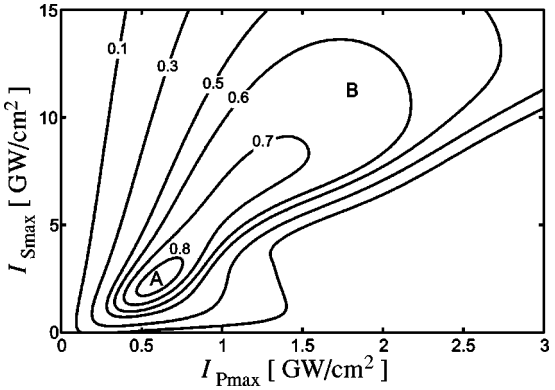

FIG. 3. Contour plot of the final excited-state population, $P_e(\infty)$, for different peak intensities $I_{P\ \max}$ and $I_{S\ \max}$ of the *P* and *S* pulses. The pulse parameters are $t_S=-3$ ns, $\tau_P=1$ ns, and $\tau_S=10$ ns. For each pair of intensities the detunings Δ_P and Δ_{SP} are chosen to be the optimal values defined by Eqs. (14) and (15).

$$\tau_S = 10 \text{ ns}, \quad \tau_P = 1 \text{ ns}, \quad t_S = -3 \text{ ns}. \quad (16)$$

For each choice of $I_{P\ \max}$ and $I_{S\ \max}$ the detunings are the optimal ones defined by Eqs. (14) and (15).

Figure 4 shows a contour plot of the inversion η as a function of the two peak intensities $I_{P\ \max}$ and $I_{S\ \max}$. The pulse duration and pulse delay are the same as in Fig. 3; again the detunings were optimized for each choice of intensity. Two local maxima are evident in Fig. 4, labeled *A* and *B*. These regions are also identified in Fig. 3, although there the region *B* has no local maximum.

The local maxima of region *A* in the two figures occurs for pulse areas of about 1.6π. Because such a value does not satisfy the criterion (10), the SCRAP mechanism does not apply in this region. The absolute maximum of the final population of level *e* (see Fig. 3), approaches 86% for the particular choice $I_{P\ \max}=0.6$ GW/cm^2 and $I_{S\ \max}=2.4$ GW/cm^2 (region *A*). For these intensities the population inversion see Fig. 4) is $\eta=0.993$.

Region *B* is associated with larger pulse areas than region *A*. In Fig. 4 the local maximum of region *B* occurs for the *P*-pulse area of 5.3π, a value consistent with applicability of

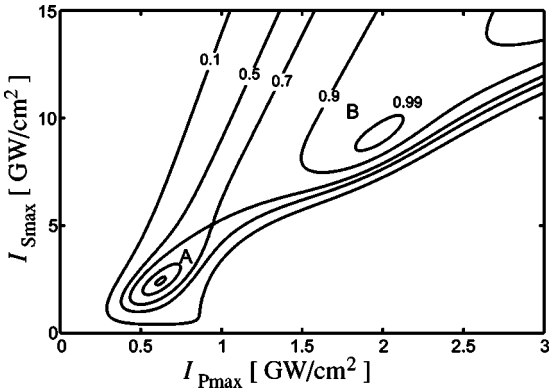

FIG. 4. Contour plot of the population inversion η for different intensities of *P* and *S* pulses. Pulse parameters are the same as in Fig. 3.

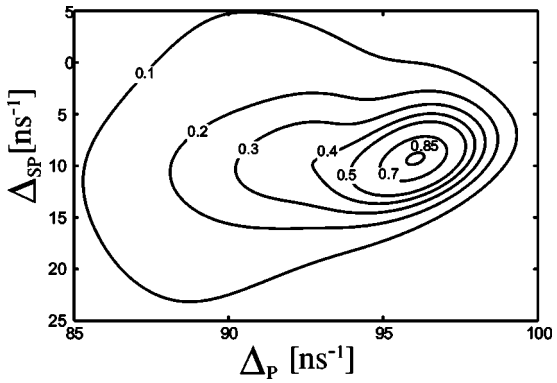

FIG. 5. Contour plot of the final population of level e as a function of detunings Δ_P and Δ_{SP}. The intensities (chosen to maximize population transfer in region A of Fig. 3), are $I_{P\,\max}=0.6$ GW/cm^2, $I_{S\,\max}=2.4$ GW/cm^2. The other parameters are those of Fig. 3.

the SCRAP procedure. Thus the letters *A* and *B* in Figs. 3 and 4 denote regions in which conditions for SCRAP are violated and obeyed, respectively. The association of regions *A* and *B* with the failure or success of SCRAP are confirmed by an examination of the time evolution of the state vector viewed in an adiabatic basis, as shown below. The contours in region *A*, where SCRAP is not effective, are more closely spaced than those of region *B*, where SCRAP contributes to population transfer. This indicates that population transfer is less sensitive to the variations of intensities when the SCRAP mechanism acts, i.e., the SCRAP mechanism contributes to robustness of population transfer.

There is a large range of intensities in the SCRAP region *B* of Fig. 4 where the inversion exceeds 90%. In the corresponding *B* region of Fig. 3 the population transfer is greater than 60%. The inversion approaches 99.998% for $I_{P\,\max}=1.96$ GW/cm^2 and $I_{S\,\max}=9.1$ GW/cm^2. The final population of level e in this case is 64%.

The contour plots of Figs. 5 and 6 confirm the suitability of the optimal detuning, Eqs. (14) and (15). Figure 5 shows the variation of the population transfer (to state e) with detunings Δ_P and Δ_{SP}, for intensities that maximize the population transfer, as expressed by Eq. (14). Figure 6 shows the

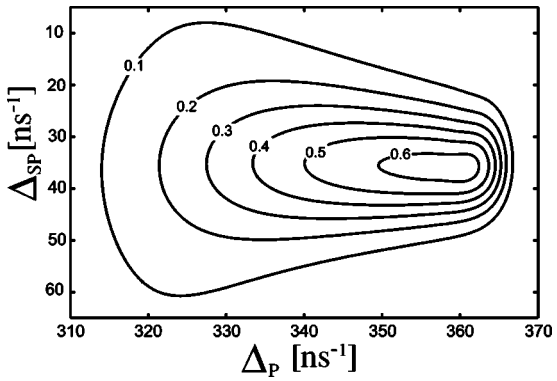

FIG. 6. Contour plot as in Fig. 5 but for region *B* and with intensities, $I_{P\,\max}=1.96$ GW/cm^2, $I_{S\,\max}=9.1$ GW/cm^2 chosen to maximize the inversion in region B of Fig. 4.

TABLE II. Parameters for maximizing inversion for region A and region B.

Parameter	Region A	Region B
$I_{P\,\max}$	0.6 GW/cm^2	1.96 GW/cm^2
$I_{S\,\max}$	2.4 GW/cm^2	9.1 GW/cm^2
$\Delta_P=\Delta_{P\,opt}$	96 ns^{-1}	360.7 ns^{-1}
$\Delta_{SP}=\Delta_{SP\,opt}$	−9.2 ns^{-1}	−35.2 ns^{-1}

variation of the inversion η with these detunings, for intensities that maximize the inversion, as expressed by Eq. (15). Table II gives the values of the intensities that maximize inversion in Fig. 4. This table also gives the optimal detunings calculated from Eqs. (14) and (15) for these intensities. The numerical values for the detunings which maximize population transfer in Fig. 5 and inversion in Fig. 6 are very close to the calculated values. The difference is less than 1 ns^{-1}.

C. Doppler effect

Examination of Fig. 5, which corresponds to regions *A* of Figs. 3 and 4 where SCRAP fails, or of Fig. 6, which corresponds to regions *B* where SCRAP succeeds, shows that the range of detunings which allow good population transfer via SCRAP is substantially larger than the range of detunings which are effective without SCRAP. These observations also lead to an estimate of the influence of Doppler broadening on the efficiency of population transfer. For a hydrogen atom moving with the velocity v the two-photon detuning Δ_P has to be replaced by the effective detuning $\tilde{\Delta}_P=\Delta_P-(4\pi/\lambda_P)v$ and Δ_{PS} by $\tilde{\Delta}_{PS}=\Delta_{PS}+(2\pi/\lambda_P-2\pi/\lambda_S)v$. Then from the contour plots on Figs. 5 and 6 we conclude that for the SCRAP region the velocity interval of effective population of the level e (larger than 50%) is about $\Delta v\simeq 400$ m/s (meaning a bandwidth of 1.7 GHz for the P laser) whereas for region *A*, where SCRAP fails, it is much smaller, $\Delta v\simeq 100$ m/s (meaning a P-field bandwidth of about 0.4 GHz).

IV. UNDERLYING POPULATION DYNAMICS

A. Adiabatic states

It is instructive to examine in some detail the time dependence of the populations in various levels to understand the concerted operation of the two mechanisms, SCRAP and LICS, in the excitation process. For this purpose we introduce three adiabatic states $\Phi_n(t)$ and the associated eigenvalues $\varepsilon_n(t)$, defined as instantaneous solutions to the time-dependent Schrödinger equation

$$\mathsf{W}(t)\Phi_n(t)=\varepsilon_n(t)\Phi_n(t). \tag{17}$$

These adiabatic states coincide with bare states in the absence of the laser fields, and so we label them using indices indicative of this connection *before* the arrival of the pulses. Using such states we write the statevector as the expansion

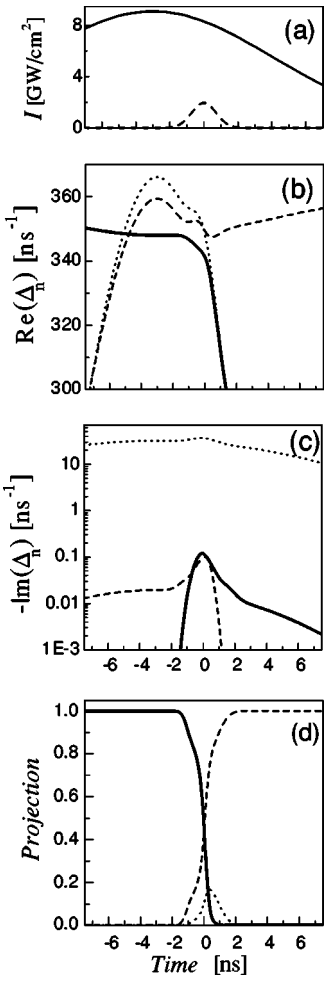

FIG. 7. Time dependence of the intensities of the *P* pulse (solid line) and *S* pulse (dashed line) (a), as well as the real (b) and imaginary (c) parts of adiabatic eigenvalues $\varepsilon_n(n=g,e,b)$. The contribution of bare states ψ_n in state Φ_g, as measured by the projection $|\langle\Phi_g(t)|\psi_n\rangle|^2$, is shown in (d). The bare states are solid line *g*, the dashed line *e*, dotted line *b*. The pulse parameters are given in Table II (region B).

$$\Psi(t) = B_g(t)\Phi_g(t) + B_e(t)\Phi_e(t) + B_b(t)\Phi_b(t). \qquad (18)$$

Because the Hamiltonian is not Hermitian, the eigenvalues are complex valued. Furthermore, the eigenvectors are not orthogonal and therefore $|B_n(t)|^2$ is not the probability of finding the system in the adiabatic state $\Phi_n(t)$ at time *t*: even if the state vector $\Psi(t)$ coincides with $\Phi_e(t)$, there is some probability to find an atom in $\Phi_g(t)$ or $\Phi_b(t)$. This fact does not affect the mathematics we use here.

B. SCRAP regime, region B

We first illustrate the dynamics during the interaction as deduced from examining the adiabatic eigenvalues. As an example we consider the SCRAP regime (region *B* of Figs. 3 and 4), choosing parameters of laser pulses that produce maximum inversion. The pulse parameters are given in Table II.

Figure 7(a) shows the time dependence of the intensities of the *P* pulse (solid line) and the a *S* pulse (dashed line). These pulses induce time variation in the real and imaginary parts of the adiabatic eigenvalues $\varepsilon_n(t)$, as shown in Figs. 7(b) and 7(c), respectively. Two of the adiabatic states, $\Phi_g(t)$ and $\Phi_e(t)$, undergo slow probability loss (of at most 0.12 ns^{-1}), while $\Phi_b(t)$ undergoes rapid probability loss (the loss rate is about 35 ns^{-1}). This difference in loss rates is a manifestation of the coherent population trapping effect that underlies LICS: the coupling of two discrete states through the continuum leads to the formation of "dark" and "bright" eigenstates with very different ionization losses. In an ideal case, when condition (15) is fulfilled for all times, the probability of ionization of the dark state decreases to zero. The existence of this dark state underlies the possibility for ionization suppression by LICS and population transfer through the continuum [18,20]. In our case one more discrete state is involved in the interaction. As a result we have two eigenstates with small ionization loss and one with large loss.

The adiabatic state $\Phi_g(t)$, which undergoes relatively slow probability loss, is connected with the ground state ψ_g for early times and with the excited state ψ_e for late times [see Fig. 7(f)]. Thus if the time evolution is adiabatic there are no transitions between adiabatic states and an atom which was initially in the ground state will be found in the excited state after the interaction—the SCRAP process is active. The population transfer is not complete because of the complex nature of the eigenvalues of the effective Hamiltonian. In the adiabatic limit the population $|B_g(t)|^2$ of the adiabatic state $\Phi_g(t)$ is given by

$$B_g(t) = B_g^{(adiab)}(t) = \exp\left[-i\int_{-\infty}^{t}\varepsilon_g(t')dt'\right]B_g(-\infty). \qquad (19)$$

The consequent maximum excitation probability is

$$P_{e\,\max} = \exp\left[-2\int_{-\infty}^{\infty}\mathrm{Im}\,\varepsilon_g(t)dt\right]. \qquad (20)$$

The conditions for adiabatic evolution can be met more easily, i.e., with lower laser power, when the pulses are long, but the maximum transfer becomes smaller with an increase of the time interval during which $\mathrm{Im}\,\varepsilon_g(t)$ provides the dominant contribution to the exponent of Eq. (20). Hence *an increase of the population transfer comes at the cost of decreasing robustness*.

Figure 8(a) shows the time dependence of the adiabatic state populations as measured by $|B_g(t)|^2$ and $|B_e(t)|^2$. The values of $|B_b(t)|^2$ are all too small to be visible here (less than 10^{-4}). The values of $|B_g(t)|^2$ is very close to the ideal case of adiabatic following [short dash curve, calculated using Eq. (19)], whereas $|B_e(t)|^2$ is very small (less than 4×10^{-2}). This means that the system can be represented very well by the adiabatic state $\Phi_g(t)$.

The decrease of the population transfer efficiency for increasing pulse amplitudes, when SCRAP becomes dominant, results from an increase of the imaginary part of the corresponding eigenvalue. There are two reasons for this increase. First, two-photon ionization by the *S* field increases. Second,

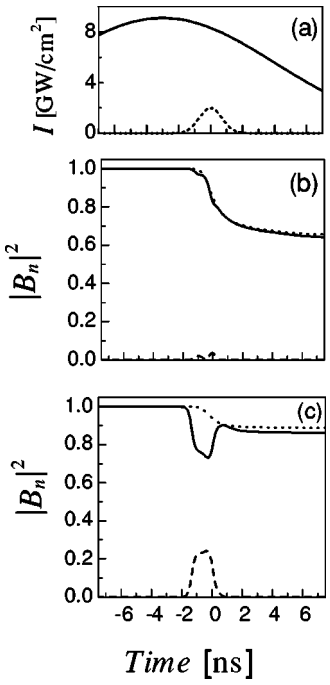

FIG. 8. Time dependence of the intensities of the *P* pulse (solid line) and *S* pulse (dashed line) (a), as well as the time dependence of the adiabatic states populations $|B_g(t)|^2$ (solid line) and $|B_e(t)|^2$ (dotted line) for (b) region *B* where SCRAP succeeds and (c) region *A* where SCRAP fails. The short dash line shows the ideal case of adiabatic following calculated using Eq. (19). The pulse parameters are given in Table II.

complete coherent suppression of ionization through LICS is possible only for static fields and detunings. Using pulsed fields with large intensity we increase the range of values of the Stark shifts, and thereby increase the ionization rate.

C. Regime where SCRAP fails, region A

Figure 8(b) illustrates the regime in which SCRAP fails. This figure shows the time dependence of $|B_g(t)|^2$ and $|B_e(t)|^2$ for the intensities and detunings given in Table II (region A). One can see here that transitions occur among adiabatic states primarily during the *P* pulse.

At the conclusion of he *P*-field interaction there is little difference between the computed populations and the ideal adiabatic following of $|B_g(t)|^2$, because the pulse intensities have been chosen to maximize population transfer. Our simulations show much more pronounced differences between the actual and the ideal adiabatic following when the intensities are far from these optimal values. Thus an increase of laser intensities leads to more robust population transfer, but this is accompanied by an increase of population loss due to imperfect LICS.

D. Robustness

For small intensities the time evolution is not adiabatic. Nevertheless, it is possible to find some intensities which maximize the population transfer (this is an analog of a π pulse but for a lossy system affected by dynamic Stark shifts). The difference in robustness for the regions where SCRAP succeeds and where it fails is evident in Figs. 3 and 4. There we observe a narrow maximum for efficient population transfer in region A and a broader dependence in region B. The difference in robustness is evident also in Figs. 5 and 6: the interval of detunings where appreciable population transfer exists is substantially different for the two regions.

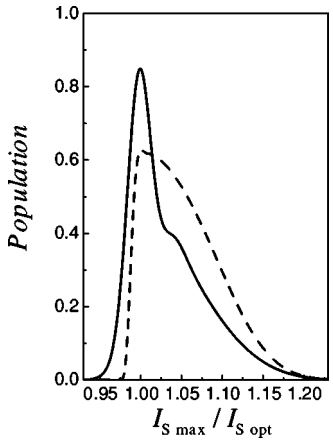

FIG. 9. The final population of the excited state, $P_e(\infty)$, as a function of the intensity of the *S* laser in units of the optimal *S*-laser intensity for fixed *P*-laser intensity and fixed detunings as given in Table II. The full line is region *A*, where SCRAP fails, dashed line is region *B*, where SCRAP succeeds.

It is important to note that in the calculations shown in Figs. 3 and 4 the detunings were adjusted to their optimal value for each pulse. In any experiment the pulse intensities fluctuate from pulse to pulse, so it is useful to see the influence of these fluctuations on the robustness of the population transfer. For both regions *A* and *B* a change of intensities with fixed static detunings will, because of the incremental Stark shifts, take the atom away from the condition for two-photon resonance. Therefore the intensity fluctuations decrease the population transfer. Figure 9 shows the population of the excited state as a function of the intensity of the *S* laser, in units of the optimal *S*-laser intensity, for fixed *P*-laser intensity and fixed detunings of both lasers, as given in Table II. We see that the population transfer efficiency is quite sensitive to fluctuations of the laser intensity. The desired stability of the laser pulse energy is about 5%. Note that the robustness with regard to intensity fluctuations is larger for the SCRAP region than for the region where SCRAP fails.

V. CONCLUSIONS

We have shown by numerical simulation studies that population transfer from the ground state of hydrogen to the metastable 2*s* state can be as high as 86%, and that population inversion between the 2*s* and 1*s* can be as high as 99%, although the two achievements do not occur for the same pulse conditions. The successful population transfer results from the concerted action of the mechanism of Stark-chirped rapid adiabatic passage (SCRAP) for population transfer and the suitable implementation of laser-induced continuum

structure (LICS) for the suppression of detrimental photoionization processes. Because SCRAP requires a suitably crafted Stark shift but the creation of pronounced LICS suffers from Stark shifts, the laser parameters (peak intensities, pulse delay and detuning) must be chosen carefully. If that is done, the optimal contributions of SCRAP and LICS to the transfer process can be realized with only two laser pulses and with intensities readily available from commercial laser systems.

ACKNOWLEDGMENTS

L.P.Y. and V.I.R. acknowledge support from the Deutsche Forschungsgemeinschaft (Grant No. 436 UKR 113/46/9) B.W.S. acknowledges support by funds from the Max-Planck-Forschungspreis 2003 awarded to K.B.

APPENDIX: THE LICS EFFECTIVE HAMILTONIAN

We consider an atom interacting with two laser fields: a P laser with amplitude $\varepsilon_P(t)$, intensity $I_P(t)$, and carrier frequency ω_P, and an S laser with amplitude $\varepsilon_S(t)$, intensity $I_S(t)$, and carrier frequency ω_S. The total electric field is

$$\mathbf{E}(t) = \mathrm{Re}[\mathbf{e}_S\varepsilon_S(t)\exp(-i\omega_S t) + \mathbf{e}_P\varepsilon_P(t)\exp(-i\omega_P t)], \tag{A1}$$

where $\mathbf{e}_j$ is a unit vector prescribing the polarization of field j. We express the state vector $|\Psi(t)\rangle$ of the atom as a combination of three particular bound states $n=g, e, b$, with energies $\{E_g, E_e, E_b\}$, together with a sum over all other bound states and an integral over continuum states, using the Dirac picture:

$$|\Psi(t)\rangle = \sum_{n=g,e,b} C_n(t)\exp(-iE_n t/\hbar)|n\rangle \tag{A2}$$

$$+ \sum_{n\neq g,e,b} A_n(t)\exp(-iE_n t/\hbar)|n\rangle \tag{A3}$$

$$+ \sum_j \int dE A_{E,k}(t)\exp(-iEt/\hbar)|E,k\rangle, \tag{A4}$$

where $|E,k\rangle$ is a continuum state with energy E. The label k identifies different possible continua having the same energy.

Starting from the time-dependent Schrödinger equation we adiabatically eliminate all amplitudes except those of the particular states g, e, b [21,22,25,26]. In so doing, we obtain effective interactions, and dynamic energy shifts, expressible in terms of a polarizability tensor [25],

$$\mathsf{Q}_{mn}(\omega) = \sum_k \frac{\langle m|\mathbf{d}|k\rangle\langle k|\mathbf{d}|n\rangle}{E_k - E_m - \hbar\omega} + \int dE \sum_k \frac{\langle m|\mathbf{d}|E,j\rangle\langle E,j|\mathbf{d}|n\rangle}{E - E_m - \hbar\omega}, \tag{A5}$$

where $\mathbf{d}$ is the dipole-moment operator. The continuum integral includes the resonance energy $E=E_m+\hbar\omega$, whose singularity is dealt with by breaking the integration into a nonsingular principal value part (denoted by $\mathcal{P}$) and a resonant part (yielding the transition rate of a Fermi golden rule),

$$\mathrm{Re}\,\mathsf{Q}_{mn}(\omega) = \sum_j \frac{\langle m|\mathbf{d}|j\rangle\langle j|\mathbf{d}|n\rangle}{E_j - E_m - \hbar\omega} + \mathcal{P}\int dE \sum_k \frac{\langle m|\mathbf{d}|E,k\rangle\langle E,k|\mathbf{d}|n\rangle}{E - E_m - \hbar\omega},$$

$$\mathrm{Im}\,\mathsf{Q}_{mn}(\omega) = \sum_k \pi\langle m|\mathbf{d}|E = E_m + \hbar\omega, k\rangle\langle E = E_m + \hbar\omega, k|\mathbf{d}|n\rangle. \tag{A6}$$

The adiabatic elimination yields a three-state time-evolution equation, which may be written [22]

$$\frac{d}{dt}\begin{bmatrix} C_g(t) \\ C_e(t) \\ C_b(t) \end{bmatrix} = -\frac{i}{2}\begin{bmatrix} 2S_g(t) + 2\Delta_P & \Omega_P(t) & 0 \\ \Omega_P(t) & 2S_e(t) - i\Gamma_e(t) - i\gamma_e & -(i+q)\Omega_{SP}(t) \\ 0 & -(i+q)\Omega_{SP}(t) & 2S_b(t) + 2\Delta_{PS} - i\Gamma_b(t) - i\gamma_b \end{bmatrix}\begin{bmatrix} C_g(t) \\ C_e(t) \\ C_b(t) \end{bmatrix}. \tag{A7}$$

The theoretical ionization rates $\Gamma_n(t)$ and Stark shifts $S_n(t)$ appearing here are obtainable by summing partial rates and shifts:

$$\Gamma_n(t) = \sum_{k,\alpha} \Gamma^{(k)}_{n\alpha}(t), \quad S_n(t) = \sum_\alpha S_{n\alpha}(t), \tag{A8}$$

where $\Gamma^{(k)}_{n\alpha}(t)$ is the ionization rate from state n to continuum k caused by laser α,

$$\Gamma^{(j)}_{n\alpha}(t) = \frac{\pi}{2\hbar}|\mathcal{E}_\alpha(t)|^2 \sum_{\alpha,k} |\langle n|\mathbf{e}_\alpha\cdot\mathbf{d}|E = \hbar\omega_\alpha - E_n, k\rangle|^2, \tag{A9}$$

and $\hbar S_{n\alpha}(t)$ is the dynamic Stark shift of the energy of state n produced by laser α:

$$\hbar S_{n\alpha}(t) = -\frac{1}{4}|\mathcal{E}_\alpha(t)|^2 \mathbf{e}_\alpha\cdot[\mathsf{Q}_{nn}(\omega_\alpha) + \mathsf{Q}_{nn}(-\omega_\alpha)]\cdot\mathbf{e}^*_\alpha. \tag{A10}$$

The quantity

$$\Omega_{SP}(t) \equiv \sqrt{\Gamma_{eP}^{(k)}(t)\Gamma_{bS}^{(k)}(t)} \tag{A11}$$

is an effective Rabi frequency for the two-step transition from the state e to the state b with intermediate population of the continuum states k with energy $E \simeq \hbar\omega_P + E_e \simeq \hbar\omega_S + E_b$. The Fano q parameter appearing here can be evaluated from the expression [21,22]

$$q\Omega_{SP}(t) = \frac{1}{2}|\mathcal{E}_P(t)\mathcal{E}_S(t)|\mathbf{e}_p \cdot [\mathsf{Q}_{eb}(\omega_P) + \mathsf{Q}_{be}(-\omega_S)] \cdot \mathbf{e}_S^*. \tag{A12}$$

The two-photon detuning Δ_{PS} is given by

$$\hbar\Delta_{PS} \equiv \hbar(\omega_P - \omega_S) - (E_b - E_e). \tag{A13}$$

Equation (A7) is usable for any two excited states; hence there appears a constant loss rate γ_n for each state, expressing the rate at which spontaneous emission removes population from state n.

The effective Hamiltonian implied by Eq. (A7) requires dynamic Stark shifts $S_n(t)$, photoionization rates $\Gamma_n(t)$, spontaneous emission rates γ_n, an effective Rabi frequency $\Omega_{SP}(t)$, and the Fano parameter q. In principle, all of these quantities can be calculated if the atomic wave functions are known, as they are for hydrogen.

[1] D. Landhuis, L. Matos, S. C. Moss, J. K. Steinberger, K. Vant, L. Willmann, Thomas J. Greytak, and D. Kleppner, Phys. Rev. A **82**, 022718 (2003).

[2] K. C. Harvey, J. Appl. Phys. **53**, 3383 (1982).

[3] N. E. Rothery and E. A. Hessels, Phys. Rev. A **61**, 044501 (2000).

[4] B. G. Brunetti, S. Falcinelli, E. Giaquinto, A. Sassara, M. Prieto-Manzanares, and F. Vecchiocattivi, Phys. Rev. A **52**, 855 (1995).

[5] S. Jonsell, A. Saenz, P. Froelich, R. C. Forrey, and R. C. Dalgarno, Phys. Rev. A **65**, 042501 (2002).

[6] R. C. Forrey, R. Coté, A. Dalgarno, S. Jonsell, A. Saenz, and P. Froelich, Phys. Rev. Lett. **85**, 4245 (2000).

[7] T. C. Killian, D. G. Fried, L. Willmann, D. Landhuis, S. C. Moss, T. J. Greytak, and D. Kleppner, Phys. Rev. Lett. **81**, 3807 (1998).

[8] B. L. Donnally, T. Clapp, W. Sawyer, and M. Schultz, Phys. Rev. Lett. **12**, 502 (1964).

[9] L. P. Yatsenko, B. W. Shore, T. Halfmann, K. Bergmann, and A. Vardi, Phys. Rev. A **60**, R4237 (1999).

[10] T. Rickes, L. P. Yatsenko, S. Steuerwald, T. Halfmann, B. W. Shore, N. V. Vitanov, and K. Bergmann, J. Chem. Phys. **113**, 534 (2000).

[11] L. P. Yatsenko, N. V. Vitanov, B. W. Shore, T. Rickes, and K. Bergmann, Opt. Commun. **204**, 413 (2002).

[12] N. V. Vitanov, M. Fleischhauer, B. W. Shore, and K. Bergmann, in *Advances in Atomic Molecular and Optical Physics*, edited by B. Bederson and H. Walther (Academic, New York, 2001), Vol. 46, pp. 55–190; N. V. Vitanov, T. Halfmann, B. W. Shore, and K. Bergmann, Annu. Rev. Phys. Chem. **52**, 763 (2001).

[13] Y. P. Malakyan and R. G. Unanyan, Opt. Commun. **126**, 38 (1996).

[14] A. K. Popov, V. V. Kimberg, and T. F. George, Phys. Rev. A **68**, 033407 (2003).

[15] M. Shapiro, Z. D. Chen, and P. Brumer, Chem. Phys. **217**, 325 (1997).

[16] U. Fano, Phys. Rev. **124**, 1866 (1961).

[17] L. Armstrong, Jr., B. L. Beers, and S. Feneuille, Phys. Rev. A **12**, 1903 (1975); Y. Heller, I. and A. K. Popov, Kvantovaya Elektron. (Moscow) **3**, 1129 (1976); [Sov. J. Quantum Electron. **6**, 606 (1976)]; Y. I. Heller and A. K. Popov, Opt. Commun. **18**, 7 (1976); **18**, 449 (1976); Y. I. Heller and A. K. Popov, Phys. Lett. **56A**, 453 (1976); Y. I. Geller and A. K. Popov, Sov. J. Quantum Electron. **6**, 606 (1976); G. Alber and P. Zoller, Phys. Rev. A **27**, 1713 (1983).

[18] Y. I. Heller, V. F. Lukinykh, A. K. Popov, and V. V. Slabko, Phys. Lett. A **82**, 4 (1981); S. S. Dimov, Y. I. Heller, L. I. Pavlov, A. K. Popov, and K. V. Stamenov, Appl. Phys. B: Photophys. Laser Chem. **30**, 35 (1983); Y. I. Geller and A. K. Popov, J. Sov. Laser Res. **6**, 1 (1985); S. Cavalieri, F. S. Pavone, and M. Matera, Phys. Rev. Lett. **67**, 3673 (1991); Y. L. Shao, D. Charalambidis, C. Fotakis, Z. Zhang, and P. Lambropoulos, *ibid.* **67**, 3669 (1991); O. Faucher, D. Charalambidis, C. Fotakis, J. Zhang, and P. Lambropoulos, *ibid.* **70**, 3004 (1993); O. Faucher, Y. L. Shao, D. Charalambidis, and C. Fotakis, Phys. Rev. A **50**, 641 (1993); A. Shnitman, I. Sofer, I. Golub, A. Yogev, M. Shapiro, Z. Chen, and P. Brumer, Phys. Rev. Lett. **76**, 2886 (1996); R. Eramo, S. Cavalieri, L. Fini, M. Matera, and L. F. DiMauro, J. Phys. B **30**, 3789 (1997); S. Cavalieri, R. Eramo, L. Fini, M. Materazzi, O. Faucher, and D. Charalambidis, Phys. Rev. A **57**, 2915 (1998).

[19] T. Halfmann, L. P. Yatsenko, M. Shapiro, B. W. Shore, and K. Bergmann, Phys. Rev. A **58**, R46 (1998); L. P. Yatsenko, T. Halfmann, B. W. Shore, and K. Bergmann, *ibid.* **59**, 2926 (1999).

[20] P. E. Coleman and P. L. Knight, J. Phys. B **15**, L235 (1982); G. X. Li and J. S. Peng, Opt. Commun. **138**, 59 (1997).

[21] B.-N. Dai and P. Lambropoulos, Phys. Rev. A **36**, 5205 (1987); Phys. Rev. A **39**, 3704(E) (1989).

[22] P. L. Knight, M. A. Lauder, and B. J. Dalton, Phys. Rep. **190**, 1 (1990).

[23] M. Dörr, O. Latinne, and C. J. Joachain, Phys. Rev. A **55**, 3697 (1997).

[24] L. P. Yatsenko, R. G. Unanyan, K. Bergmann, T. Halfmann, and B. W. Shore, Opt. Commun. **135**, 406 (1997).

[25] B W. Shore, *The Theory of Coherent Atomic Excitation* (Wiley, New York, 1990).

[26] Z. Deng and J. H. Eberly, J. Opt. Soc. Am. B **2**, 486 (1985).